CONCLUSION

In this paper, we have presented the original results of a comparative analysis of different types of coaxial excitation of the TM_{01l} mode in a cylindrical cavity containing a spherical lossy load (a fruit) and considered various factors influencing on the efficiency of coupling and the patterns of dissipated power. It appears that due to its rather wide resonant characteristics (not too sensitive to minor changes of some design parameters), the 915-MHz structure shown in Figure 3 may be chosen as a suitable basic unit of a practical device for thermal processing of various spherical fruits in the temperature range at least from 20° to 60°C if they possess approximately the same diameter.

The presented approach, which takes care of both energy coupling and patterns of dissipated power, can be used in a similar manner for electromagnetic modeling of realistic systems of microwave thermal processing. Through a series of virtual experiments, it can be remarkably beneficial to the engineering design of complex microwave applicators.

REFERENCES

1. T.V. Chan and H.C. Reader, Understanding microwave heating cavities, Artech House, Boston–London, 2000.
2. Y. Hassler and L. Johansen, Microwave heating of fused quartz to high temperatures in the fabrication process of optical fibers, Proc 18th Euro Microwave Conf, Madrid, Spain, 1988, pp. 613–618.
3. J. Jow, M.C. Hawley, M. Finzel, J. Asmussen, Jr., H.H. Lin, and B. Manring, Microwave processing and diagnostics of chemically reacting materials in a single-mode cavity applicator, IEEE Trans Microwave Theory Tech MTT-35 (1987), 1435–1443.
4. S. Isaksson and A. Bondeson, Aspects of continuous tubular microwave heating, Proc 7th Conf Microwave and HF Heating, Valencia, Spain, 1999, 209–212.
5. P.J.B. Clarricoats and B.C. Taylor, Evanescent and propagating modes of dielectric-loaded circular waveguides, Proc IEE 111 (1964), 1951–1956.
6. K.A. Zaki and A.E. Atia, Modes in dielectric-loaded waveguides and resonators, IEEE Trans Microwave Theory Tech MTT-31 (1983), 1039–1045.
7. V.V. Yakovlev, Examination of contemporary electromagnetic software capable of modeling problems of microwave heating, M. Willert-Porada (Ed.), Advances in microwave and radio frequency processing, Springer, New York, 2005, pp. 178–190.
8. P.S. Moral, J.M. Catalá-Civera, E. de los Reyes, and D. Sánchez-Hernández, Electromagnetic design of a microwave applicator for industrial rice disinfection processes, Proc 7th Conf Microwave and HF Heating, Valencia, Spain, 1999, pp. 477–480.
9. S. Kalhori, N. Elander, J. Svennebrink, and S. Stone-Elander, A re-entrant cavity for microwave-enhanced chemistry. J Microwave Power Electromagn Energy 38 (2003), 125–135.
10. J.M. Catalá-Civera, S. Giner-Maravilla, D. Sánchez-Hernández, and E. de los Reyes, Pressure-aided microwave rubber vulcanization in a ridged three-zone cylindrical cavity, J Microwave Power Electromagn Energy 35 (2000), 92–104.
11. J.N. Ikedia, J.D. Hansen, J. Tang, S.R. Drake, and S. Wang, Development of a saline water immersion technique with RF energy as a postharvest treatment against codling moth in cherries, Postharvest Biology Tech 24 (2002), 25–37.
12. C.-C. Lu, H.-Z. Li, and D. Gao, Combined electromagnetic and heat-conduction analysis of rapid rewarminging of cryopreserved tissues, IEEE Trans Microwave Theory Tech MTT-48 (2000), 2185–2190.
13. QuickWave-3D™, QWED Sp. z o. o., ul. Piêkna 64a m 11, 00-672 Warsaw, Poland, http://www.qwed.com.pl/.
14. S. Wang, J. Tang, J.A. Johnson, E. Mitcham, J.D. Nahsen, G. Hallman, S.R. Drake, and Y. Wang, Dielectric properties of fruits and insects pests as related to radio frequency and microwave treatments, Biosystems Engg 85 (2003), 2003.

MIMO SPACE-TIME CODING FOR DIFFUSE OPTICAL COMMUNICATION

Matt Garfield, Chao Liang, Timothy P. Kurzweg, and Kapil R. Dandekar
Department of Electrical and Computer Engineering
Drexel University
3141 Chestnut St.
Philadelphia, PA 19104

Received 29 November 2005

ABSTRACT: *A multiple input, multiple output (MIMO) diffuse optical communications link is implemented and evaluated using a 2 × 2 Alamouti-type space-time coding scheme to increase link performance beyond that of single input, single output (SISO) and multiple input, single output (MISO) systems. We present a representative profile of received power versus distance, and comparative bit-error probability performance.* © 2006 Wiley Periodicals, Inc. Microwave Opt Technol Lett 48: 1108–1110, 2006; Published online in Wiley InterScience (www.interscience.wiley.com). DOI 10.1002/mop.21558

Key words: *MIMO; diffuse optics; space-time coding; infrared communications; free-space optics*

INTRODUCTION

Modern office environments have an expanding demand for wireless local area networks (LANs). Traditionally, these networks have been implemented using radio frequency (RF) communication methods. RF networks provide a wide coverage area, supporting mobile users at data rates up to hundreds of Mb/s. However, the broad coverage of RF networks presents security risks and significant interference concerns. Due to these limitations, the use of RF radiation is strictly regulated, thus severely restricting the available bandwidth. In this paper, we present the use of infrared (IR) diffuse optical signaling to overcome the inherent limitations of RF communications. While IR-based communication systems are not typically employed due to received signal-power limitations, alignment issues, and low data rates, we propose the use of multiple input, multiple output (MIMO) signal-processing techniques to overcome these limitations and enable high-performance diffuse optical links. Using IR light as the transmission medium, we create a picocellular coverage area within an indoor office-type environment using a standard ceiling as a diffusing surface. IR light is constrained by the physical boundaries of a room, creating a tightly contained coverage area that presents a significant security and frequency/network planning advantage over RF-based networks. This IR system also reduces interference concerns that allow the IR band to be unregulated worldwide, thus creating the potential for virtually unlimited bandwidth [1]. By incorporating multiple transceiver elements and MIMO STC techniques, we hope to achieve data rates that meet or exceed current RF LANs with significantly improved security and ease of deployment.

MIMO OPTICAL SPACE-TIME CODING

Transmitting IR light onto a diffusing surface, such as an office ceiling, causes it to scatter, thus creating various multipath components. Previous diffuse optical MIMO link research has incorporated multispot diffusion methods to reduce the reception of multipath components. Our work is unique in that we have employed MIMO STC techniques to productively utilize the "crosstalk" and multipath-signal environment that generally limits conventional optical communication systems. Adapting the 2 × 1 Alamouti-type encoding method, we derive a maximum-likelihood

decision rule for a 2×2 diffuse optical MIMO configuration. Specifically, for $i \in \{1, 2\}$, we can choose $x_i = \hat{x}_i$ iff:

$$(\tilde{x}_i - \hat{x}_i)^2 + (h_{1,1}^2 + h_{2,1}^2 + h_{1,2}^2 + h_{2,2}^2 - 1)\hat{x}_i^2 \leq (\tilde{x}_i - x_i)^2 + (h_{1,1}^2 + h_{2,1}^2 + h_{1,2}^2 + h_{2,2}^2 - 1)x_i^2, \quad (1)$$

where x_i is the transmitted on–off keyed symbol, $\tilde{x}_i$ is the maximum-likelihood decision statistic, and $\hat{x}_i$ is the estimated transmitted signal at the receiver. The propagation channel coefficient from the b^{th} transmitter to the a^{th} receiver is given by $h_{a,b}$. In contrast to RF-MIMO systems, the channel coefficients for an IR-MIMO system are real, nonnegative values.

Our method uses a training period to characterize the communications channel and calculate the instantaneous channel coefficients ($h_{a,b}$) with each packet transmission. During the training period, each transmitter element is driven individually. These alternating pilot signals allow the receiver array to estimate all of the channel coefficients used in Eq. (1). After the training sequence, the Alamouti encoded payload is simultaneously sent by both independent and spatially separated transmitters. The transmitted signals utilize unique, but correlated, paths to each of the spatially separated receiver elements. Bit values are decoded by applying the channel coefficients determined during the training period and received signal to the decision rule in Eq. (1).

To evaluate the bit-error-rate performance, we derive the bit-error probability conditioned on channel knowledge (CBEP) obtained during the training interval for the maximum likelihood receiver from Eq. (1):

$$\text{CBEP} = Q\left(\sqrt{\frac{E_b}{2N_0}\mathbf{h}^T\mathbf{h}}\right), \quad (2)$$

where $Q(x)$ is the Gaussian Q-function, E_b/N_0 is the total bit energy to noise ratio, and $\mathbf{h} = [h_{1,1}, h_{1,2}, h_{2,1}, h_{2,2}]^T$.

We can evaluate the potential of differing levels of transmit diversity by considering a variable number of channel coefficients in the decision rule in Eq. (1) and the CBEP in Eq. (2). For example, a conventional single input, single output (SISO) architecture can be evaluated using only the $h_{1,1}$ terms of the two equations. Similarly, the $h_{1,1}$ and $h_{2,1}$ terms can be used to consider a multiple input, single output (MISO) architecture. To provide a fair comparison between SISO and MISO/MIMO configurations, power normalization was performed by scaling E_b to ensure that total transmit power was constant for both single- and multiple-transmitter configurations.

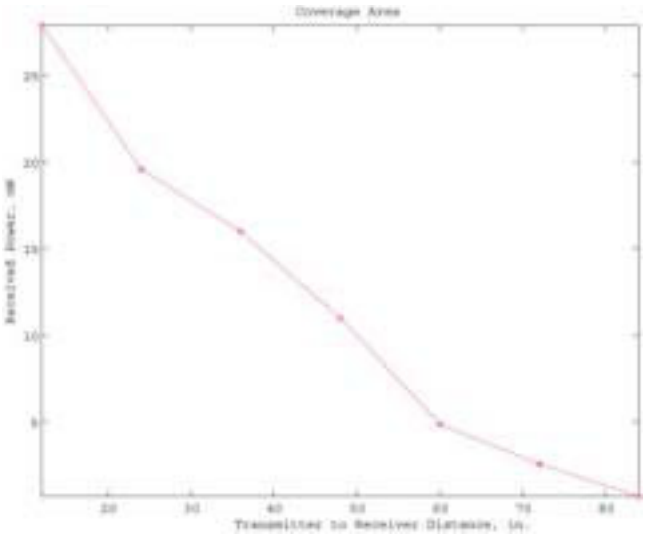

Figure 1 Plot of received power vs. distance using 120 mW per transmitter element. [Color figure can be viewed in the online issue, which is available at www.interscience.wiley.com]

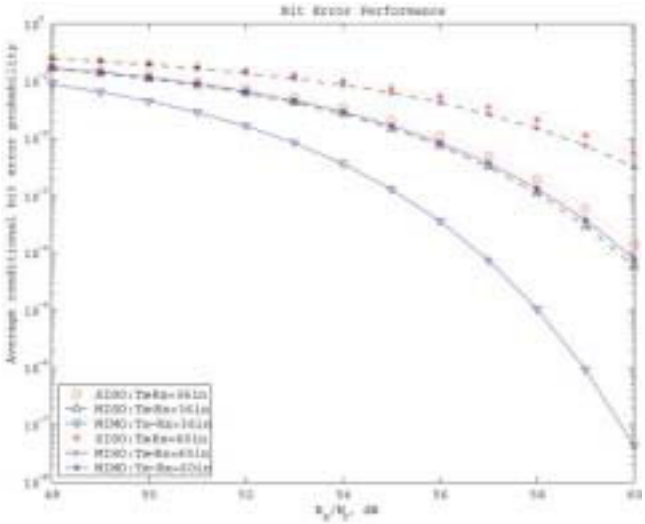

Figure 2 Comparison of bit-error performance with different transmitter-to-receiver distances and variable levels of transmit and receive diversity. [Color figure can be viewed in the online issue, which is available at www.interscience.wiley.com]

EXPERIMENTAL TESTBED

We have developed a flexible experimental diffuse optical MIMO testbed with which we can test the performance of the MIMO STC. The baseband of our system is a software-defined radio making use of high-speed arbitrary-waveform generators and digitizers from National Instruments. Infrared emitting diodes (Vishay TSHF5400) and photodetectors (Vishay TESP5700) were used to implement the transmitter and receiver arrays, respectively. We have performed several channel sounding experiments to characterize the diffuse optical MIMO channel and evaluate the performance of the testbed, implementing the methods described above. Figure 1 shows a plot of the received power versus transmitter-to-receiver distance. In Figure 2, we compare the CBEP for several test cases: a 1×1 SISO link, a 2×1 MISO link, and a 2×2 MIMO link. The experiments were conducted in an indoor laboratory environment with no special preparation or treatment on the walls or ceilings to enhance the propagation of multipath-signal components. Although the results presented in this paper were conducted without the presence of ambient lighting, the qualitative results remain unchanged when ambient is introduced. The results are discussed below.

RESULTS

The coverage-area plot shown in Figure 1 shows that we can maintain sufficient received power levels to reliably detect a pilot signal from a transmitter with an output power of 120 mW at a distance of 7 feet. Beyond the 7-foot threshold, the receiver was no longer able to detect a pilot signal over the ambient noise. This is consistent with our notion of a secure picocellular coverage area. The size of the coverage area could be increased by increasing the transmitter power or through the use of better amplification at the

receiver. Current research is focused on the construction of more sophisticated transceiver electronics in order to allow for larger (and adjustable) access-point coverage areas. In the relatively short-range indoor office environment in which the experiments were conducted, we observed that the measured channel coefficients, **h**, could be modeled as correlated Gaussian random variables.

In Figure 2, we observe the effects of transmitter-to-receiver distance on the CBEP over the range of E_b/N_0 measured during the field experiments. We also compare the CBEP performance of the diffuse optical link under SISO, MISO, and MIMO configurations in order to quantify the benefits of additional levels of system complexity. As expected, when the transmitter-to-receiver distance is fixed, there is increased CBEP performance when switching from SISO to MISO to MIMO configurations. However, the benefit of using MISO over SISO is relatively small. This result can be explained by noting that total transmit power was held constant for single- and multiple-transmitter configurations. Furthermore, these results show that diffuse optical space-time coding with transmit diversity alone is not enough to yield an appreciable performance increase. The use of both transmit and receive diversity in a MIMO configuration, however, improves CBEP performance given equal levels of transmitted signal power. As Figure 2 shows, MIMO processing allows the larger transmitter-to-receiver link to outperform a conventional SISO link of a smaller distance. Thus, MIMO techniques can significantly increase the effective range of a diffuse optical access point without the need for additional signal power.

CONCLUSION

Diffuse optical links provide a more secure alternative to traditional RF systems by providing a tightly contained wireless coverage area. By applying MIMO space-time coding to diffuse optical communication links, we can utilize the various multipath components to reduce the CBEP, thereby increasing the achievable data rate. Using our experimental testbed, we verified our MIMO space-time code to show a proof-of-concept diffuse optical MIMO wireless link providing a secure picocellular coverage area with a 7-foot radius. We demonstrated that the application of our 2×2 MIMO STC outperforms both the SISO and MISO configurations. Further research in this area will consider the impact of different transceiver array geometries (spacing, orientation, and so forth), error-correcting codes, and adaptive power control on the performance of the MIMO free-space optical link.

ACKNOWLEDGMENTS

This material is based upon work supported by the National Science Foundation under grant nos. 0524200 and 0322795. National Instruments has provided equipment donations supporting this research.

NEW PLANAR SLOTTED-PATCH RESONATOR FOR MINIATURIZED BANDPASS FILTER APPLICATIONS

Wen-Jian Zhang and Zheng-Fan Li
Department of Electronic Engineering
Shanghai Jiao Tong University
Shanghai 200240, China

Received 30 November 2005

ABSTRACT: *A new planar slotted-patch resonator is proposed for RF and microwave bandpass filter design. The novelty of the proposed resonator is that it can reduce the size of the filter significantly. It is found that the resonant frequency of the resonator is reduced (for example, by 61%). A dual-mode filter operating at 2.39 GHz with 1.7% bandwidth and a three-pole bandpass filter operating at 2.375 GHz with 8.8% bandwidth are designed and fabricated. The measured results agree very well with the full-wave EM simulation.* © 2006 Wiley Periodicals, Inc. Microwave Opt Technol Lett 48: 1110–1112, 2006; Published online in Wiley InterScience (www.interscience.wiley.com). DOI 10.1002/mop.21557

Key words: *slotted-patch resonator; dual-mode filter; bandpass filter; miniaturization; multilayer*

1. INTRODUCTION

Modern microwave communications systems, such as satellite and mobile communications systems, challenge bandpass filters with more stringent requirements—low loss, compact size, and low cost. Since the concept of microstrip dual-mode bandpass filter was proposed in the early 1970s by Wolff [1], it has been widely used in wireless communications systems requiring high-quality narrowband bandpass filters.

The square-patch resonator has been widely applied to antenna design [2]. However, it is difficult to be used in the design of planar circuits (for example, filters) because of the high radiation loss and low Q-factor, as compared to its ring counterpart. A patch resonator etched by a pair of crossed slots was proposed in [3] for the design of a size-reduced CP patch antenna. In [4], the structure was successfully utilized in the design of a dual-mode bandpass patch filter by suitably selecting the unequal cross-slot lengths along the two orthogonally diagonal planes, demonstrating simultaneous size and loss reduction. In [5], an inductively loaded cross-slotted patch resonator was presented to build up a miniaturized dual-mode bandpass filter and its size was reduced to $\lambda/4$. In [6], one miniaturized slotted-patch resonator was designed by the optimal use of a vertical coupling mechanism and transverse cuts and utilized to realize three- and five-pole bandpass filters via the novel 3D deployment of single-mode patch resonators.

In this paper, we form square slots in addition to the crossed slots, as illustrated in Figure 1, to further reduced the size and radiation loss of the patch resonator. A comparative study is first carried out to exhibit the resonant frequency of several types of slotted patch resonator. A dual-mode filter with patch size of less than $\lambda/5$ is designed. Then a three-pole bandpass filter is implemented in a multilayer configuration. The coupling of the feeder-to-patch and patch-to-patch are largely raised, thus giving the potential of widening the passband. The filters are fabricated and measured to validate the predicted performance.

2. MINIATURIZED SLOTTED PATCH RESONATOR

Here we study the resonance behaviors of the four single-mode patch resonators shown in Figure 2, namely, resonators (a)–(d),